Innovation
2020; 1(1): 6-17
http://www.sciencepublishinggroup.com/j/innov
doi: 10.11648/j.innov.20200102.11

Water Wave Energy Harvesting Power Producing Stations as the Only Solution Avoid Coming Point of No Return

George Nerubenko*, David Flowers, Cyril Nerubenko, Dmitry Gurevich

NER*MAR Limited, Toronto, Canada

Email address:
gneru@hotmail.com (G. Nerubenko), df42@brighthouse.com (D. Flowers), info@mega-automation.ca (C. Nerubenko), dgurevych@mega-automation.ca (D. Gurevich)

*Corresponding author

To cite this article:
George Nerubenko, David Flowers, Cyril Nerubenko, Dmitry Gurevich. Water Wave Energy Harvesting Power Producing Stations as the Only Solution Avoid Coming Point of No Return. *Innovation*. Vol. 1, No. 2, 2020, pp. 6-17. doi: 10.11648/j.innov.20200101.12

Received: December 10, 2020; **Accepted**: December 22, 2020; **Published**: December 31, 2020

Abstract: The newly invented and patented as US Patent on energy harvesting power producing apparatus is considered in the paper. This device could have the various applications. The authors consider the most effective application – to use it as the water wave energy harvesting power producing station. Based on analysis of numerous facts, evidences, articles, observations it is confirmed that the point of no return has high probability to happen in coming 20 – 30 years. It means that at a point of no return the catastrophic impact of the damaged Mother Nature would ruin the mankind. In coming point of no return the increase of our planet temperature; increase the climate change, increase of CO_2, etc., will happen. Then the people will begin die due to dirty atmosphere, harmful and dangerous water and poisoned food. The authors provide the proof that the water wave energy harvesting power producing stations can guarantee only solution avoid coming point of no return. The proposed device is the vibration energy harvesting damper that is adjustable to a broad range of frequencies. The device includes a support structure that is securable to a vibrating object, a tuned mass retained by the support structure and movable in a rectilinear direction, a magnet vibrationally coupled to and spaced apart from the tuned mass, a coil surrounding the magnet, and at least one biasing assembly connecting two or more of the support structure, the tuned mass and the magnet. The at least one biasing assembly includes a fixed biasing member and an adjustable biasing member arranged in parallel. The adjustable biasing member is configured to adjust the combined stiffness coefficient of the biasing assembly. There were analytical study, design, manufacturing and test provided for proposed advance schemes of the water wave energy harvesting power producing station. It was concluded that such station would be effective to replace fossil-fuel station and solar panel and wind turbine stations.

Keywords: Point of No Return, Water Wave Energy Harvesting Power Producing Station, "Green" Electricity

1. Introduction

The usage and exploitation of our Earth resources cause the troubles to all components of an environment. For instance, for water resources the clean solutions could be achieved when exploiting technology is safe and specially designed meeting environment requirement. Some examples illustrate the necessity of such approach. Evaluation of sea polluting by damaged oil tankers had the following numbers: Exxon Valdez Tanker disaster (1989) was $ 6 Billion, and Prestige Tanker was $ 4 Billion in 2002. Sea polluting by damaged BP Deepwater Platform 2010 in Mexican Gulf was over $ 42 Billion. The sources of oil spills such as damages, holes, cracks, etc of tankers and oil platforms are targeting. By the way BP disaster changed (among others) the surface properties of Gulf Stream, covering the surface by film of oil, which (as one of the results) changed the reflective ability of surface causing a change of the temperature of Gulf Stream. The Gulf Stream influences radically on the climate changes of the east coast of North America from Florida to Newfoundland. Other example-there is a solution to make clean atmosphere – install the filter on each muffler, exhaust pipe, chimney of industrial plant, chimney of power station, etc.; but such filters are expensive and they must be replaced every month at least. It is not good for profit, for money in people, businesses and industry budgets; they want to save money as much as possible. Such activity leads to a Point of No Return, when the catastrophic impact of the damaged Mother Nature would ruin the mankind. The implementation

of the water wave energy harvesting power producing stations based on authors US Patent [1] can kill the problem in embryo and provide the solution to avoid coming Point of No Return.

2. Examples of Underwater Petroleum Catastrophes and Statistics of Oil Spills

The operation of technique in marine oil industry is accompanied by some natural malfunctions, accidents, wrecks, breakages, damages which occur from time to time. The amount and scope of damages could be different and should have random probability. But it is obvious that the bigger number of industrial objects would have the higher probability of non proper functioning, damages, breakages, and so on. Only for the Gulf of Mexico the approximate estimates indicate that there are 3600 production platforms, 300 drilling rigs, and 2500 vessels on a daily basis. EPA confirms that there are 20000 oil spills reported in the Gulf of Mexico yearly. Unfortunately the huge disasters and catastrophes happen in marine oil industry. The Exxon Valdez oil spill occurred in Prince William Sound, Alaska, on March 24, 1989, when Exxon Valdez, an oil tanker struck Prince William Sound's Bligh Reef at 12:04 a.m. local time and spilled at least 41000 m_3 of crude oil over the next few days, fouling about 2100 kilometers of coastline [3, 4]. The remote location of the spill and a delayed and inadequate response from Exxon and Trans-Alaska Pipeline operator ALYESKA made matters even worse. The oil slick had spread over 8000 square kilometers. The authors of stated: "Exxon was not prepared for a spill of this magnitude- nor were Alyeska, the State of Alaska, or the federal government [3]. It is clear that the planning for and response to the Exxon Valdez incident was unequal to the task. Contingency planning in the future needs to incorporate realistic worst-cast scenarios and to include adequate equipment and personnel to handle major spills."

On November 13, 2002, while the Greek-operated, single-hulled oil tanker Prestige was carrying 77000 metric tons of cargo of heavy fuel oil, one of its twelve tanks burst during a storm in northwestern Spain [5]. Thinking that the ship would sink, the captain called for help from Spanish rescue team, with the expectation that the vessel would be brought into harbor. However, pressure from local authorities forced the captain to steer the embattled ship away from the coast and head to French coast. Reportedly after pressure from the French government, the vessel was once again forced to change its course and head south into Portuguese waters. Fearing for its own shore, the Portuguese authorities promptly ordered its navy to prevent it from approaching further. The integrity of the oil tanker was quickly deteriorating, and during the storm it was reported that a 12 - meter section of the starboard hull had broken off, releasing a substantial amount of oil. At around 8:00 a.m. on November 19, the ship split in half. It sank the same afternoon, releasing over 76000 m^3 of oil into the sea. After the sinking, the wreck continued leaking oil. It leaked approximately 125 tons of oil a day, polluting the seabed and contaminating the coastline. The affected area was a very prominent ecological region, supporting coral reefs and many species of sharks, birds and fishes. The heavy coastal pollution forced the local government to suspend offshore fishing for six months.

The *BP Deepwater Horizon* oil pollution disaster was caused by an explosion on the Deepwater Horizon offshore oil platform about 80 kilometers southeast of the Mississippi River delta on April 20, 2010 [6, 7]. This resulted in 11 worker fatalities and a massive petroleum release. The *Deepwater Horizon* sank in about 1500 meters of water on April 22, 2010. After a series of failed efforts to plug the leak, BP said on July 15 that it had capped the well, stopping the flow of oil into the Gulf of Mexico for the first time in 86 days. Totally this subsea drilling system discharges petroleum of approximately 780000 m3 to U.S. waters. The oil slick produced by the Deepwater Horizon oil spill covered as much 75000 square kilometers. Such surface slick threatened the ecological systems and the economy of the entire Gulf Coast region. The underwater damages following by oil spills were the common characteristics of all these abovementioned catastrophes.

There are several societies, institutions, organizations collecting the informational data about oil spills. It is very difficult to accumulate all statistical data in one body because of different nature of spills, different objects, and different ways of recording and reporting, variety of areas, different tasks and addresses of reporting and so on. There is a report where the data of largest tanker spills are collected; the data are based on reports of oil spills from one tanker and the volume of spilled oil from one tanker had to be over 37854 m^3 [8]. Data were collected from 1960 to 1999. Figure 1 shows the treated oil spill volume numbers (in m^3) plotted for interval of years 1960 – 1996. The reported data are presented by squared points interconnected with solid blue curved line. The trend-line approximation is plotted as solid red straight line. The graphical analysis indicates that the trend-line has the slight declining tendency. The absolute numbers of largest tanker spills are slightly reduced in 1960 – 1999 period from 86000 m^3 to 85000 m^3.

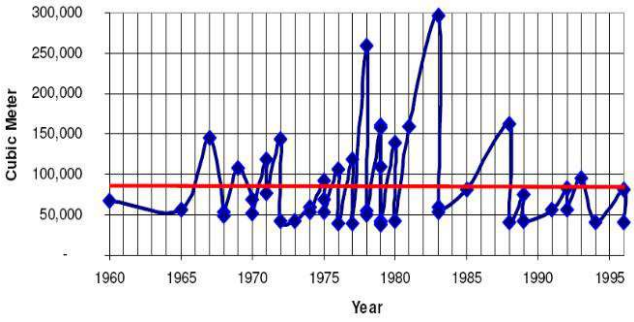

Figure 1. *Largest tanker spills in 1960-1996. All spills of 37854 cubic meters or more.*

ITOPF. was underlined that usually a few very large spills were responsible for a high percentage of oil spilt [9]. For instance, in four year period 2010-2013 there have been 28 spills of 7 tones and over, resulting in 22000 tones of petroleum lost. 90% of this volume was spilt in 8 incidents. It

could be stated that it is clear evidence of sharp declining of tanker's oil spill tendency line starting from 2000.

It is noted in BOEM Report that there is a steady reduction in the number of offshore accidents reported by several studies (if to exclude the BP Deepwater well spill in the average and median spill sizes), the size of spills from platforms to be smaller than those from tankers [10]. For example, assuming that for 1964 -2013 interval the relative volume of oil spills from offshore platforms was 100%, and for last 15 years this number was reduced to 29.5%. Unfortunately the oil spill estimates are subjected by selected method of study [11, 12]. There is no 100% proof that the situation with oil spills in the offshore platform industry is radically improved. Stanislav Patin has pointed out that the most typical causes of accidents "include equipment failure, personnel mistakes, and extreme natural impacts (seismic activity, ice fields, hurricanes, and so on) [13]. Their main hazard is connected with the spills and blowouts of oil, gas, and numerous other chemical substances and compounds. The environmental consequences of accidental episodes are especially severe, sometimes dramatic, when they happen near the shore, in shallow waters, or in areas with slow water circulation. Broadly speaking, two major categories of drilling accidents should be distinguished. One of them covers catastrophic situations involving intense and prolonged hydrocarbon gushing. These occur when the pressure in the drilling zone is so high that usual technological methods of well muffling do not help.

Drilling accidents are usually associated with unexpected blowouts of liquid and gaseous hydrocarbons from a well as a result of encountering zones with abnormally high pressure. No other situations but tanker oil spills can compete with drilling accidents in frequency and severity." Environmental impacts may arise at all stages of offshore platform activities, including initial exploration, production and final decommissioning. However the total amounts of underwater spills are very high and numbers of accidents are still significant.

One of the goals of petroleum engineers is a reduction of the environmental impacts of the petroleum industry on the marine environment, specifically through implementation of advanced underwater technique.

3. Examples of Destroying Earth Atmosphere and Moving to Point of No Return

There is a simple solution to keep atmosphere clean, this solution is to install the catalytic converter on each automobile muffler, to install the filter on each exhaust pipe, on chimney of industrial plant, on chimney of electric power station and etc.; but such filters are very expensive and they must be replaced every month at least. Hence, it is not good for profit, for money in people's, businesses and industry budgets; they want to save money as much as possible.

In 2015 the US Environmental Protection Agency (EPA) found that many VW cars being sold in America had a fake software in diesel engines that could detect when they were being tested, changing the performance accordingly to improve results. The German car giant has since admitted cheating emissions tests in the US. The EPA said in November that it had found the same test-cheating software on additional VW and Audi diesel models and on a Porsche model. The agency said it covered about 85,000 cars sold in the US. Financially, VW will be recalling millions of cars worldwide and has set aside about $7.2 billion to cover costs. But that's unlikely to be the end of the financial impact. The EPA has the power to fine a company up to $37,500 for each vehicle that breaches standards - a maximum fine of about $18 billion. Moreover, the costs of possible legal action by car owners and shareholders cannot be estimated with any certainty at this time. This disgraceful act happen because the company cultivated a culture of fear and deceit that led to its unethical actions: scare tactics imposed on employees; self-interested decision-making; and a total disregard for the driving public. No doubt the pressure was linked to a desire to maximize revenue and produce financial results that met or exceeded financial analysts' earnings expectations. It is important to understand that all German companies have two boards: the management board, led by the CEO, runs the business day-to-day, and above it the supervisory board, to which the CEO reports. The supervisory board can hire and fire management board members and must sign off on major strategic decisions. It has been reported that staff members in engine development felt pressure from the management board to find a cost effective solution to develop clean diesel engines for the US market. Rather than telling VW's management board the rules could not be adhered to, staff members in engine development decided to push ahead with manipulation, according to a German Publication, Sueddeutsche Zeitung.

Another example - at the beginning of previous century the majority of cars were electric.

Next example is from history of Toronto city transport. It was proposed to substitute trolley bus system by fueled busses. Between 1947 and 1993, the TTC operated a trolley bus system on medium ridership routes. In 1947, the TTC created four trolley bus routes (Lansdowne, Ossington, Annette, and Weston Road) in the west end that replaced streetcar routes…The last trolley buses ran in 1993 on the Bay and Annette routes. Rather than replacing the aging trolley bus infrastructure, the TTC decided to use buses to replace the trolley bus fleet. In January 1960, the General Motors "New Look" buses went into service. As earlier New Looks were retired they in turn would be replaced by newer versions of the New look model, with the result that the model would serve Toronto for over 50 years. In 1966, plans were made to replace all streetcar routes with buses in the next 20 years.

Hansen, J., Ruedy, R., Sato, M. & Lo, K. have addressed the questions about perception and reality of global warming [14]. Satellite-observed night lights are used to identify measurement stations located in extreme darkness and adjust temperature trends of urban and periurban stations for non-climatic factors, verifying that urban effects on analyzed global change are small. Because the GISS analysis combines available sea surface temperature records with meteorological

station measurements, we test alternative choices for the ocean data, showing that global temperature change is sensitive to estimated temperature change in polar regions where observations are limited. We use simple 12 month (and $n \times 12$) running means to improve the information content in our temperature graphs. Contrary to a popular misconception, the rate of warming has not declined. Global temperature is rising as fast in the past decade as in the prior 2 decades, despite year - to - year fluctuations associated with the El Niño - La Niña cycle of tropical ocean temperature. Record high global 12 month running mean temperature for the period with instrumental data was reached in 2010.

Serreze, M. C. & Barry, R. G. have demonstrated, that the past decade has seen substantial advances in understanding Arctic amplification — that trends and variability in surface air temperature tend to be larger in the Arctic region than for the Northern Hemisphere or globe as a whole [15]. We provide a synthesis of research on Arctic amplification, starting with a historical context and then addressing recent insights into processes and key impacts, based on analysis of the instrumental record, modeling studies, and paleoclimate reconstructions. Arctic amplification is now recognized as an inherent characteristic of the global climate system, with multiple intertwined causes operating on a spectrum of spatial and temporal scales. These include, but are not limited to, changes in sea ice extent that impact heat fluxes between the ocean and the atmosphere, atmospheric and oceanic heat transports, cloud cover and water vapor that alter the longwave radiation flux to the surface, soot on snow and heightened black carbon aerosol concentrations. Strong warming over the Arctic Ocean during the past decade in autumn and winter, clearly associated with reduced sea ice extent, is but the most recent manifestation of the phenomenon. Indeed, periods of Arctic amplification are evident from analysis of both warm and cool periods over at least the past three million years. Arctic amplification being observed today is expected to become stronger in coming decades, invoking changes in atmospheric circulation, vegetation and the carbon cycle, with impacts both within and beyond the Arctic. The main conclusions are - Temperature changes in the Arctic tend to exceed those for the globe as whole. This phenomenon is termed Arctic amplification. Arctic amplification has many causes operating on different time and space scales. Recent Arctic amplification is strongly linked to declining sea ice extent. Arctic amplification is expected to strengthen in coming decades. Impacts of Arctic amplification will extend well beyond the Arctic region.

Moon, T. A. et al. have found that the arctic land ice is melting, sea ice is decreasing, and permafrost is thawing [16]. Changes in these Arctic elements are interconnected, and most interactions accelerate the rate of change. The changes affect infrastructure, economics, and cultures of people inside and outside of the Arctic, including in temperate and tropical regions, through sea level rise, worsening storm and hurricane impacts, and enhanced warming. Coastal communities worldwide are already experiencing more regular flooding, drinking water contamination, and coastal erosion. The authors describe and summarize the nature of change for Arctic permafrost, land ice, and sea ice, and its influences on lower latitudes, particularly the United States. The authors emphasize that impacts will worsen in the future unless individuals, businesses, communities, and policy makers proactively engage in mitigation and adaptation activities to reduce the effects of Arctic changes and safeguard people and society.

C Arden Pope 3rd, Richard T Burnett, Michelle C Turner, Aaron Cohen, Daniel Krewski, Michael Jerrett, Susan M Gapstur, Michael J Thun have underlined that the Lung Cancer and Cardiovascular Disease (CVD) mortality risks increase with exposure to fine particulate matter < 2.5 μm in diameter ($PM_{2.5}$) from ambient air pollution [17]. Recent research indicates that the exposure-response relationship for CVD is nonlinear, with a steep increase in risk at low exposures and flattening out at higher exposures. Comparable estimates of the exposure-response relationship for lung cancer are required for disease burden estimates and related public health policy assessments.

The analysis of provided examples and studies tells that it must be stated that avidity, greed, voracity ruins the Earth's atmosphere and that provokes the catastrophic changes in climate, and as side effect leads to Lung Cancer and Cardiovascular Disease (CVD).

4. Selection of Advanced Technology

There is a package of the descriptions and applications of invented water wave energy harvesting power producing station (WWEHPPS) [1, 18]. The core idea of proposed station is schematically shown in Figure 2. It must be mentioned that there are a lot of other variants of proposed station. Generally speaking the station contains (see Figure 2) the floating Master Boat 1 which is in maritime area with proper weather conditions. The Master Boat is equipped by instruments, gauges, tools, devices, control systems, apparatus, meters, mechanisms on-board batteries for station functioning. Cable 2 has two functions: mechanical connection to buoy 3 (to change position of buoy, and / or load buoy to Master Boat deck, or upload buoy from the deck to water) and electric connection to buoy 3. It could be several buoys in line parallel to Master Boat board for increasing power output of a station. It could be also several lines of buoys parallel to Master Boat board for increasing power output of a station between buoys 3 and 4. Cable 5 has also two functions like cable 2. Cable 6 is positioned on seabed (ocean floor) and could deliver electricity to ground, for instance to battery station / local station 7, which could be equipped by a post 10 for delivering the electricity to a grid 8, a cable 9 is connected to a grid. The reasonable length of Master Boat 1 could be about 100 - 120 m. So the first line of buoys (parallel to board) could consist of 50 buoys 3. The number of lines could be up to 100. It gives the possibility to form a huge power station. If to select buoys producing 100 kW power, the total capacity of proposed floating station would be 500 MW.

The compressed overall description of presented US Patent is: "A vibration energy harvesting damper (VEHD) that is adjustable to a broad range of frequencies of vibration is

provided. The VEHD includes a support structure that is securable to a vibrating object, a tuned mass retained by the support structure and movable in a rectilinear direction, a magnet vibrationally coupled to and spaced apart from the tuned mass, a coil surrounding the magnet, and at least one biasing assembly connecting two or more of the support structure, the tuned mass and the magnet. The at least one biasing assembly includes a fixed biasing member and an adjustable biasing member arranged in parallel. The adjustable biasing member is configured to adjust the combined stiffness coefficient of the biasing assembly".

For understanding the main characters of the buoy's internal arrangements the Figure 3 depicts one of the versions of patented scheme. The springing element 202 having stiffness coefficient c_2 is serially connected to electromagnetic spring 278 (having equivalent quasi-stiffness coefficient e_{27}), so it is the serial connection of these springs. The coefficient e_{27} could be varied using signals from unit 222. It allows get the values of the equivalent stiffness coefficient of combined mechanical spring - electromagnetic spring arrangement 202 – 208, in significantly broad range but less than c_2.

The electromagnetic spring arrangement 208 (having equivalent quasi-stiffness coefficient e_{20}, the coefficient e_{20} could be varied using signals from unit 222).

Also it is possible to activate the parametric resonance in scheme, by time variation of coefficient e_{20} and e_{27} to get the frequency ω R of that variation equals to 2o/n, where n=1, 2, 3…, and o is the natural frequency of vibrations of 201. Parametric resonance brings to more amplitude of magnet vibrations, and that leads to more electric energy generation. All provided solutions are applicable to combined mechanical spring - electromagnetic spring arrangements 209 and 210. Ability to get parametric resonance allows getting larger amplitudes of vibration for a magnet 205 comparing to regular usual resonance, and so to increase the produced electrical energy.

On top of Figure 4 is a schematic view of a VEHD having a friction reduction unit, generally identified by reference character 320. The VEHD 320 is the same as the VEHD 220, except for the shape 920, while the magnets 928 and the coils 930 generally form an energy harvester. The VEHD 920 may further comprise a plurality of sensors 936, such as accelerometers, for controlling the VEHD 920, as described below. The casing 924 is configured to retain the various components of the VEHD 920 and is configured to securely attach to the vibrating object 922. The casing 924 is formed of a non-magnetic material, such as non-magnetic metal, plastic or other suitable material. The casing 924 may be cylindrically shaped or may be another suitable shape, as will be appreciated. Although a casing 924 is shown and described herein, it will be appreciated by those skilled in the art that other suitable support structures may be used, such as a frame. The tuned mass 926 is configured to provide vibration damping to the object 922 and to amplify the vibrations of the magnets 928 within the coils 930. The tuned mass 926 is constrained to f the casing and the tuned mass and the configuration of one of the biasing assemblies. Similar to VEHD 220, the VEHD 320 is connected to a vibrating object 322 and comprises a casing 324, a tuned mass 326, a magnet 328, a coil 330, a plurality of biasing assemblies 332 and a guide 334. The tuned mass 326 and the magnet 328 are retained by the casing 324 and are movable in a rectilinear direction, along the guide 634. The plurality of biasing assemblies 332 are connected between the casing 324, the tuned mass 326 and the magnet 328 and vibrationally couple the connected elements, such that the vibration of each one of the coupled elements influences the vibration of the other coupled elements. The coil 330 surrounds the magnet 328 and is secured to the casing 324, for example by being embedded in the casing 324.

The version shown in Figure 4 allows keep better than described above. It is an enlarged fragmentary view in the middle of Figure 4 of a portion of a tuned mass and a cantilever beam passing there through, from the VEHD. The bottom view of Figure 4 is a schematic view of the motion of a point of contact on the tuned mass from the VEHD.

Totally Figure 4 shows embodiment of a VEHD generally identified by reference character 920. The VEHD 920 is configured to provide both vibration damping and energy harvesting, over a broad range of frequencies. The VEHD 920 is configured to promote parametric resonance to increase energy harvesting, as described below. The VEHD 920 is attached to a vibrating object 922 and comprises a casing 924, a tuned mass 926, a pair of magnets 928, a pair of coils 930, a biasing assembly 932, a guide 934 and a pair of cantilever beams 988. The tuned mass 926 and the magnets 928 are retained by the casing 924. The tuned mass 926 is moveable in a rectilinear direction, along the guide 934, and the magnets 928 are movable in a transverse direction. Each of the magnets 928 is movable within a respective one of the coils 930. The transverse direction is generally perpendicular to the rectilinear direction, which is the vertical direction on top view of Figure 4. The biasing assembly 932 is connected between the casing 924 and the tuned mass 926 and vibrationally couples the casing 924 and the tuned mass 926, such that the vibration of the casing 924 influences the vibration of the tuned mass 926 and vice versa. Each of the cantilever beams 988 is connected between the casing 924 and one of the magnets 928 and passes through the tuned mass 926. The cantilever beams 988 vibrationally couple the magnets 928 to the tuned mass 926, such that the vibration of the tuned mass 926 influences the vibrations of the magnets 928, as described below. The cantilever beams 988 further vibrationally couple the magnets 928 to the casing 924, such that the vibration of the casing 924 influences the vibrations of the magnets 928. The coils 930 surround the magnets 928 and are secured to the casing 924. As will be appreciated, the tuned mass 926, the magnets 928, the biasing assembly 932 and the cantilever beams 988 generally form a vibration damper in the VEHD move in the rectilinear direction (i.e. in a single direction, such as the vertical direction in Figure 4) by the guide 934. The tuned mass 926 has a mass that is sufficient to reduce undesired vibration in the object 922. The tuned mass 926 includes a pair of slots 990. Each of the cantilever beams 988 extends through a respective one of the

slots 990 in the tuned mass 926. Each of the slots 990 includes at least one clamp 992 that slidingly engages the cantilever beam 988 extending through the slot 990 (as shown in Figure 4). Each of the clamps 992 is movable within its respective slot 990 between an uppermost position (as shown at the top of Figure 4) and a lowermost position (as shown at the bottom of Figure 4). Each of the slots 990 includes at least one drive mechanism 994 that can be used to change the position of the guide 992 along the cantilever beam 988 within the slot 990. In this embodiment the drive mechanism 994 includes a motor and gears (not shown). In alternative embodiments, the drive mechanism 994 may be electromagnetically driven or driven by other suitable means. The tuned mass 926 is formed of a non-magnetic material, such as a non-magnetic metal, and may be cylindrically shaped or another suitable shape, as will be appreciated. The magnets 928 are configured to provide vibration damping to the object 922 and are configured to generate a changing magnetic flux when vibrating within the VEHD 920. Each of the magnets 928 is secured to a free end of one of the cantilever beams 988. The magnets 928 move in the transverse direction (e.g. a generally horizontal direction in Figure 4) within the coils 930. The magnets 928 are formed of a permanent magnetic material, such as an alloy of neodymium, and have sufficient magnetic field strength to induce a useful electrical current in the coils 930. Each of the magnets 928 may be a single unitary magnet or may be an array of individual magnets. The magnets 928 are of equal weight and configuration. The magnets 928 are horizontally aligned with the same poles facing each other (e.g. the north pole of one magnet 928 faces the north pole of the other magnet 928, as shown in Figure 4) to generate a repulsive force between the magnets 928. During operation, the magnets 928 vibrate oppositely in the transverse direction (e.g. the generally horizontal direction in Figure 4), which is defined as the y-axis in this embodiment. Accordingly, as one of the magnets 928 (m_3) moves in a positive y-direction, the other magnet 928 moves in a negative y-direction. The position of one of the magnets 928 can be denoted by $y_3(t)$ and the position of the other magnet 928 can be denoted by $y_4(t)$. The opposing vibrations of the magnets 928 will generally produce opposite forces acting on the casing 924, which helps to mitigate any transverse vibrations from the magnets 928 being transmitted to the casing 924 and the object 922. The coils 930 are configured to produce the useful electrical current when exposed to the changing magnetic flux generated by the magnet 928. The coils 930 are secured within the casing 924 in a position surrounding the magnets 928 and terminate in a pair of electrical contacts for connecting to a power system or other electrical load. Each of the coils 930 comprises a number of turns for generating the useful electrical current when exposed to the changing magnetic flux. The coils 930 are formed of an electrically conductive material, such as copper wire, which may be coated to prevent short circuiting of the coil 930. The biasing assembly 932 is the same as the biasing assembly 232a, described above, and comprises a fixed biasing member 938 and an adjustable biasing member 940, which are arranged in parallel. As described above, the adjustable biasing member 940 comprises a pair of electromagnetic arrangements. The fixed biasing member 938 is configured to provide a generally fixed stiffness coefficient, and the adjustable biasing member 940 is configured to provide an adjustable stiffness coefficient. The guide 934 is configured to constrain the movement of the tuned mass 926 to a rectilinear direction (e.g. the vertical direction in Figure 4). A frequency of vibration ωN for the magnet 928 attached to the corresponding cantilever beam 988 will be equal to:

$$\omega N=\sqrt{c3/m3}$$

If the natural frequency of the tuned mass 926 vibration is the same as the casing 924 and the object 922 vibration, denoted by ω_0 then the vibration of the point of contact (p.C) can be represented by the formula $a\sin\omega_0 t$ (as shown in Figure 4), where a is the amplitude of these vibrations and where a/L is significantly less than 1. Accordingly, the stiffness coefficient c_3 would oscillate over time as defined by the equation:

$$c_3(t)=c_3(t)[1-3(a/L\sin\omega_0 t]$$

Parametric resonance in the vibrating magnets 928 attached to the corresponding cantilever beams 988 occurs when the frequency of vibration ω of the tuned mass 926 is equal to $2\omega N/n$, where n=1, 2, 3... and where ωN is the natural frequency of vibration of one of the magnets 928 attached to the corresponding cantilever beam 988, as set out above. Controlling the frequency of vibration of the tuned mass 926 to maintain parametric resonance, based on the above equations, can help to increase the amplitude of vibration of the magnets 928 within the coils 930 and, accordingly, can help to increase the amount of electrical energy generated by the VEHD 920. The differential equation describing the dynamic behavior of the magnet mass m_3 is

$$m_3\, x_3``+ B_3x_3`+c_3[1-3(a/L)\sin\omega_0 t]\, x_3=0$$

where `=d/dt, B_3 is the friction "viscocity" coefficient.

Introducing: $B_3/ m_3=b$, $c_3/m_3=k$, $q=3(a/L)$

the dynamical equation can be rewritten

$$x_3``+ bx_3`+k[1-q\sin\omega_0 t]\, x_3=0.$$

or presented as

$$x_3``+ bx_3`+ [k-e\sin\omega_0 t]\, x_3=0$$

The obtained equation is typical parametric Mathieu equation [19-21]. It is obvious that less value of the "viscosity" friction leads to bigger displacement of magnet.

Below in Figure 5 the version of patented device with possibility to make zero "viscosity" friction is presented.

Top of Figure 5 is a schematic view of a VEHD having a friction reduction unit; bottom view of Figure 5 is a graph showing a falling volt-amp characteristic from the friction reduction unit of the VEHD. So Figure 5 shows another VEHD generally identified by reference character 320. The VEHD 320 is the same as the VEHD 220, except for the shape of the casing

and the tuned mass and the configuration of one of the biasing assemblies. Similar to VEHD 220, the VEHD 320 is connected to a vibrating object 322 and comprises a casing 324, a tuned mass 326, a magnet 328, a coil 330, a plurality of biasing assemblies 332 and a guide 334. The tuned mass 326 and the magnet 328 are retained by the casing 324 and are movable in a rectilinear direction, along the guide 634. The plurality of biasing assemblies 332 are connected between the casing 324, the tuned mass 326 and the magnet 328 and vibrationally couple the connected elements, such that the vibration of each one of the coupled elements influences the vibration of the other coupled elements. The coil 330 surrounds the magnet 328 and is secured to the casing 324, for example by being embedded in the casing 324. The VEHD 320 may further comprise a plurality of sensors, such as accelerometers (not shown in Figure 5). As mentioned above, the casing 324 is the same as the casing 224, except for the shape. The portion of the casing 324 that surrounds the magnet 228 is narrower than the portion of the casing 324 that surrounds the tuned mass 326. Likewise, the tuned mass 326 is the same as the tuned mass 226, except for the shape. The tuned mass 326 is shorter and wider than the tuned mass 226. The plurality of biasing assemblies 332 is configured to bias the tuned mass 326 and the magnet 328 towards respective neutral positions (i.e. their positions before vibrating), within the casing 324. The plurality of biasing assemblies 332 comprises a first biasing assembly 332a, a second biasing assembly 332b and a third biasing assembly 332c. The second biasing assembly 332b and the third biasing assembly 332c are the same as the second biasing assembly 232b and the third biasing assembly 232c, respectively, described above. The first biasing assembly 332a is different from the second biasing assembly 332b and the third biasing assembly 332c. The first biasing assembly 332a is connected between the casing 324 and the tuned mass 326 and is configured to provide a combined stiffness coefficient, as described above. Similar to the first biasing assembly 232a, the first biasing assembly 332a comprises a fixed biasing member 338a and an adjustable biasing member 340a, which are arranged in parallel. The first biasing assembly 332a also further comprises a friction reduction unit 388 that is arranged in series with the fixed biasing member 338a. The fixed biasing member 338a is the same as the fixed biasing member 238a, except the fixed biasing member 338a is shorter. Likewise, the adjustable biasing member 340a is the same as the adjustable biasing member 240a, except the adjustable biasing member 340a is taller. Although, in other embodiments the sizes of the fixed biasing member and the adjustable biasing member may be vary. The friction reduction unit 388 is configured to reduce the friction in the first biasing assembly 332a, which can help to increase the amplitude of vibration of the tuned mass 326 and the magnet 328. As described above, increasing the amplitude of vibration of the magnet 328 can help to increase electrical power generated by the VEHD 320. The friction reduction unit 388 comprises a resistor 390, an inductor 392 and a capacitor 394 (i.e. an RLC circuit) and further comprises a semiconductor device 396 and a power source 398, all of which are electrically coupled together as shown in Figure 5. The semiconductor device 396 (such as a tunnel diode) has a falling volt-amp characteristic. Accordingly, the semiconductor device 396 exhibits a negative resistance in the forward region. This falling volt-amp characteristic could be in an S shape (as shown in Figure 5) or could be in an N shape (not shown). The value of the volt-amp characteristic ψ at operational point uoper can be tuned using the formula:

$$\psi=[(boL/b)+R]$$

where L is inductance, R is resistance, b is the coefficient of viscous friction in the first fixed biasing member 338a and bo is the coefficient of mutual conversion mechanical viscous friction into electrical system coordinates (using current base). The power source 398 in the friction reduction unit 388 can be a battery, an external power source or another suitable source of power, such as the storage 284 in the power system 262, described above. In some embodiments, the power source 398 may be one of the loads in a power system connected to the VEHD, such as one of the loads 286 in the power system 262 described above. The friction reduction unit 388 may be self-powered by the VEHD 320. Although only the first biasing assembly 332a has been shown and described above as comprising a friction reduction unit 338, it will be mentioned that in other embodiments the second biasing assembly 332b and/or the third biasing assembly 332c may include a friction reduction unit as described above. Using the MATHCAD analysis it could be possible to check the displacement of m_3. The expected displacement (stroke) was 40 mm, however the needed designed displacement should be 43 – 45 mm.

Using the MATHCAD analysis one can build the stability zones of operation for considered device (see Figure 6) [19-21]. The horizontal abscissa axis stands for parameter ***k***, and vertical ordinate axis stands for parameter ***e***. If b=0.2, the observer sees the chart as presented on top of Figure 6. If b=0, the observer sees the chart as presented on bottom of Figure 6. A comparison of these two graphs brings the observer to conclusion that the selection of b=0 makes the system more unstable. The expected displacement (stroke) was 40 mm, however the needed designed displacement should be 43 – 45 mm (see graphs of displacement and velocity in Figure 5). Also based on MATHCAD analysis one can build the stability zones of operation for considered device (see Figure 6). If b=0.2, the observer sees the chart with less un-stability zones than if b=0.

If b=0, the observer sees the chart with more un-stable zones. A comparison of these two graphs brings the observer to conclusion that the selection of b=0 makes the system more unstable.

5. Comparison of Proposed Water Wave Power Station to Other Types of Power Producing Facilities

Let's provide the analysis of presented water wave energy harvesting power producing station (WWEHPPS).

Comparing of proposed WWEPPS to two types of existing stations: so called clean stations (wind turbine and solar panel

stations), and the fossil – fuel power stations [22].

The key performances comparison of WWEPPS to wind turbine and solar panel stations are represented in Table 1.

Table 1. *Comparison of WWEPPS to wind turbine and solar panel stations.*

n/n	The current key performance metrics.		
	WWEPPS	**Solar Panel**	**Wind Turbine**
1	*Metric*		
2	1 MW Station cost		
3	$ 364,000	$ 1,100,000	$1,750,000
4	RoI – return of investment (1 MW Station)		
5	19 years	60 years	93 years

Table 2. *Comparison of WWEPPS to fossil-fuel power stations.*

n/n	The current key performance metrics.		
		WWEPPS	**CFES**
1	Initial cost for purchase and install	$182 million	$400 million
2	Annual electric output, kWh	3,810,600,000	3,066,000,000
3	Levelized cost per kWh	$ 0.94	$ 4.74
4	Net Present Worth	$358,000,000	$140,000,000

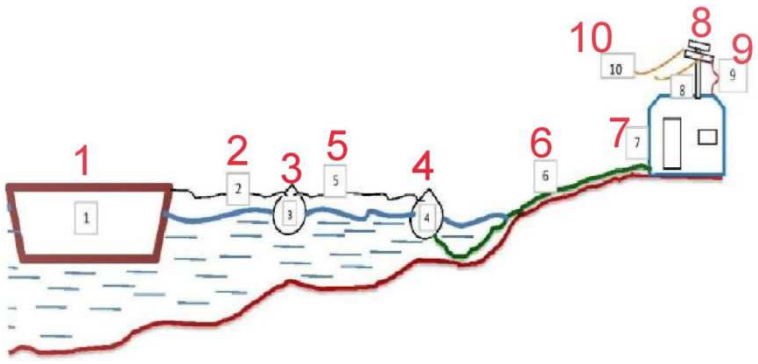

Figure 2. *Core idea of proposed station.*

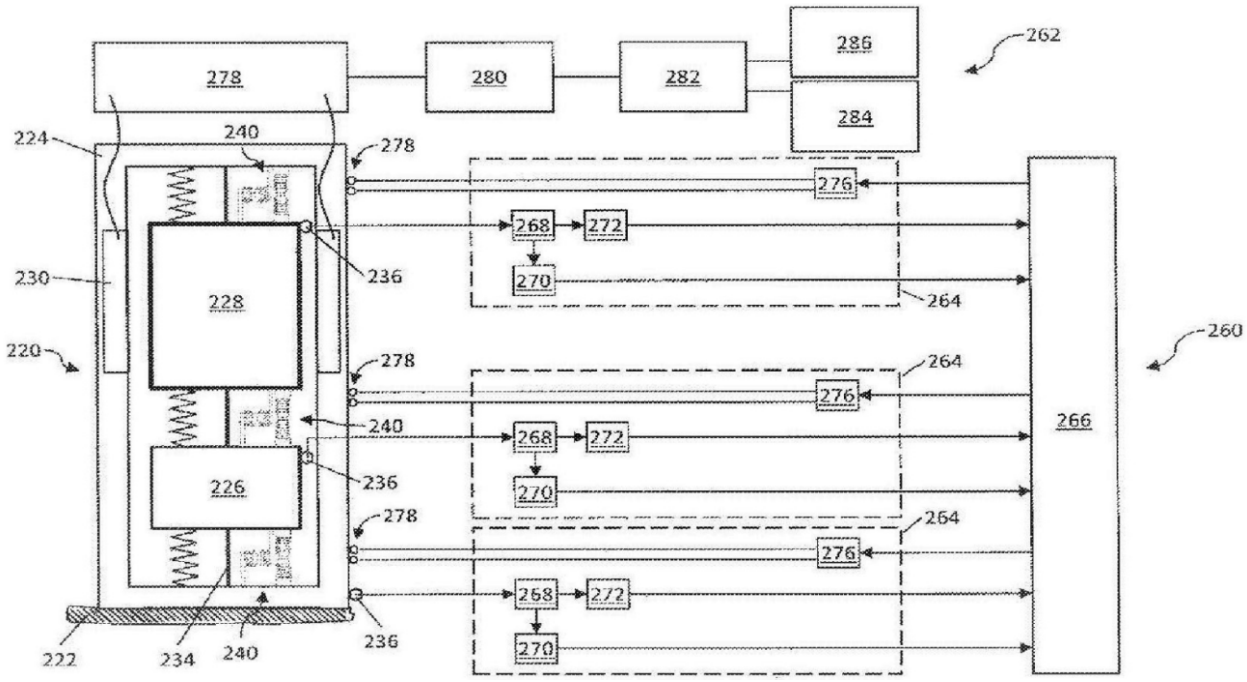

Figure 3. *Version of patented scheme.*

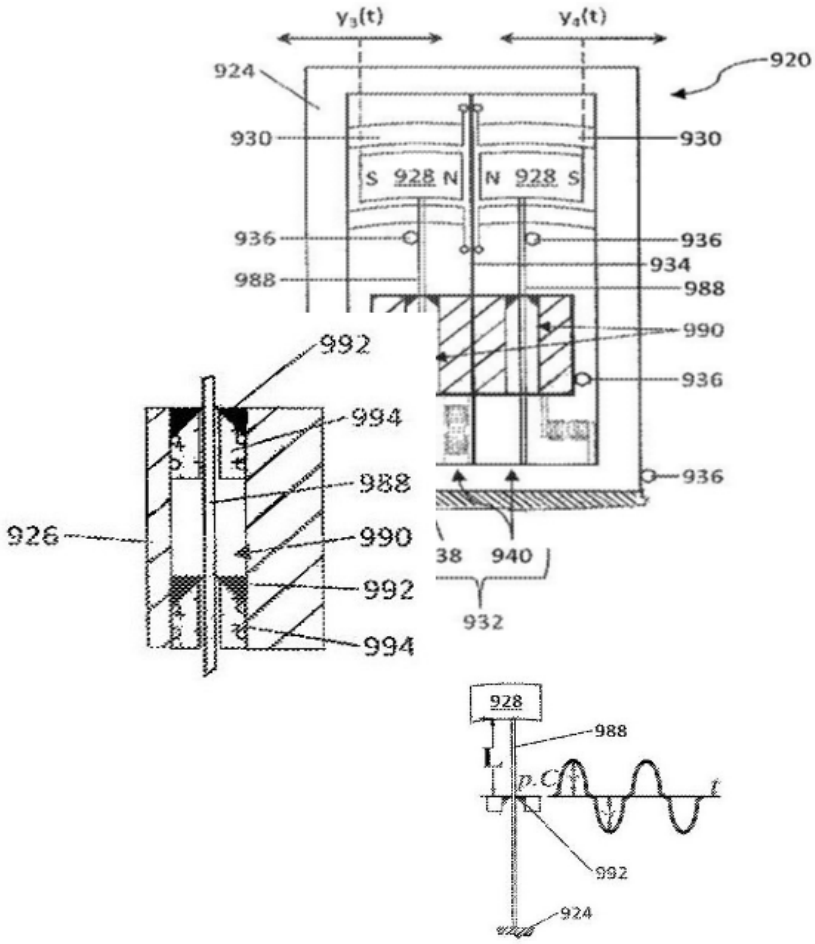

Figure 4. *Version of patented scheme.*

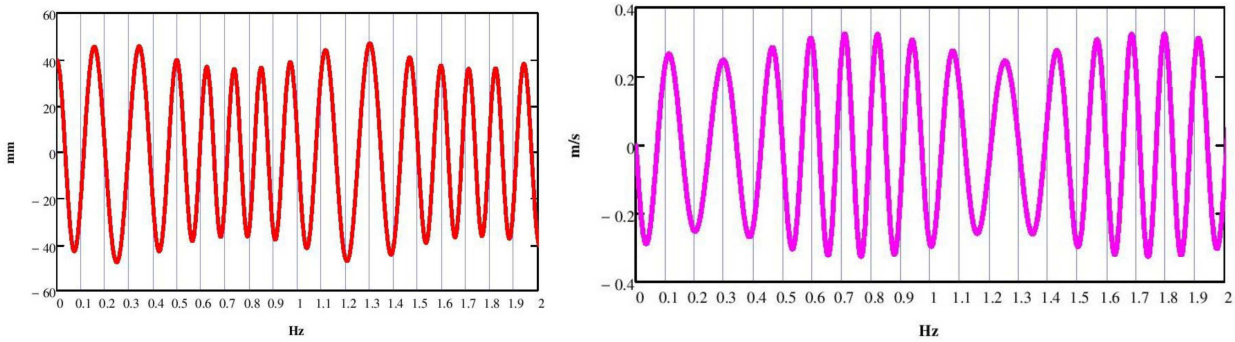

Figure 5. *Displacement and velocity of high performance VEHD.*

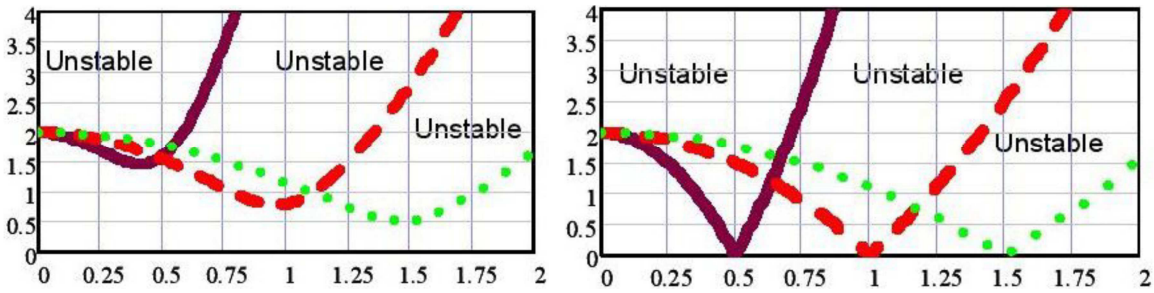

Figure 6. *Un-stable zones of high performance VEHD, Top view is when b=0.2. bottom wvie is when b=0.*

The estimates in Table 1 are based on an assumption that today's electricity cost is 21c/kWh. The truth is that solar and wind stations are subsidized by governments. So the taxpayer's money are spending for useless wind turbine and

solar panel stations, making harm and damage to environment, all these stations must be stopped immediately and replaced by the WWEPPS because WWEPPS are much better than solar or turbine stations: they are much cheaper and have much less years of return of investment.

Now let's go to Table 2 and make comparison to a typical fossil – fuel stations. A main fragment of the financial analysis is shown below for 500 MW WWEPPS.

1) WWEPPS is rated at 500 MW and has a capacity factor of 87% over 8760 operating hr/year.
2) Initial cost for purchase and install is $182 million.
3) The lifetime of the analysis is 30 years.
4) The MARR (minimum acceptable rate of return) is 8%.
5) The balance of cost is $18 million/year.

For that Capital Project

Levelized cost per kWh=0.94 c/kWh.

Net Present Worth=$358,000,000.

Annual electric output=3,810,600,000 kWh.

If the output sale price is 5.0 c/kWh, then the basic annual rough profit would be=(5.0 c – 0.94 c) * 3,810,600,000 kWh=$ 154,710,360 (compare to initial Station cost).

The explanation of terms Levelized cost and Net Present Worth are the following. Levelized Cost of Energy is a cost of generating energy (usually electricity) for a particular system. It is an economic assessment of the cost of the energy-generating system including all the costs over its lifetime: initial investment, operations and maintenance, cost of fuel, cost of capital. Typically Levelized Costs of Energy are calculated over 20 to 40 year lifetimes. Net Present Worth is an indicator of how much value an investment or project adds to the firm. In financial theory, if there is a choice between two mutually exclusive alternatives, the one yielding the higher Net Present Worth should be selected. A positive net present value indicates that the projected earnings generated by a project or investment (in present dollars) exceeds the anticipated costs (also in present dollars).

The key performances comparison of 500 MW WWEPPS and typical 500 MW Coal-Fired Electric Station (CFES) [22] are compressed in Table 2.

Encapsulating the provided financial analysis it can be stated that the 500 MW WWEPPS initial cost for purchase and install is much less than for CFES; the annual electric kW output is higher; the Levelized cost per kWh is much less; the Net Present Worth is much higher.

It is needed to mention that Canadian Government pronounced that all electric vehicles would be charged from plugs. However Canada in 2017 produced: 652 terawatt hours; and 34% of it was produced at nuclear, coal, gas/oil/others stations. There is no Falls (like Niagara Falls) in Canada for exploitation as electric power stations. Hence, it is right time to close all fossil – fuel stations promptly and substitute them by new invented WWEPPS. It could prevent coming disaster for our planet Earth – the Point of No Return. The estimates demonstrate that the cost to build WWEPPS is around 9-10 billion Canadian dollars.

The authors are using the innovative solutions for commercialization of proposed the technology to avoid the risks which are dictated by the circumstance that a station is operating in water. Water is more hostile than sun or wind, more aggressive from point of view mechanical and hydraulic impact. Hence, structures must be better protected from water penetration, mechanically stronger and have better electromechanical and control systems. Also the quality and reliability of proposed wave station is increased by assembling of 500 buoys (operating cells) of 100 kW each into one station, so, for instance, if something damaged in 1 buoy of 100 kW station – the station should produce 4,900 kW of its capacity. Other technical risks are connected to geographic (so weather) conditions, for instance the ocean in Atlantic or in Vancouver is not frozen, Lake Ontario also non frozen practically, however the lakes and rivers in middle and northern parts of Canada covered by ice for one-three winter months. Some specific technical risks could occur when the first large (100 MW and more) station would be build (so called scale effect).

However, bearing in mind that it is not needed to exclude kilometres of land (like for solar stations), so for agriculture – friendly; contrary to the massive and high-rise towers for wind turbine station - which is bad for people living nearby, for animals and birds, and stopped right now.

6. Tests of Proposed Water Wave Power Station Buoy

Based on above described schemes and recommendations the buoy was manufactured mainly in National University of Shipbuilding, Nikolaev, Ukraine (see left photo in top side of Figure 7). Practically all metallic parts (outer and inner) were manufactured in University. The buoy was located and in University's water station in South Bug River.

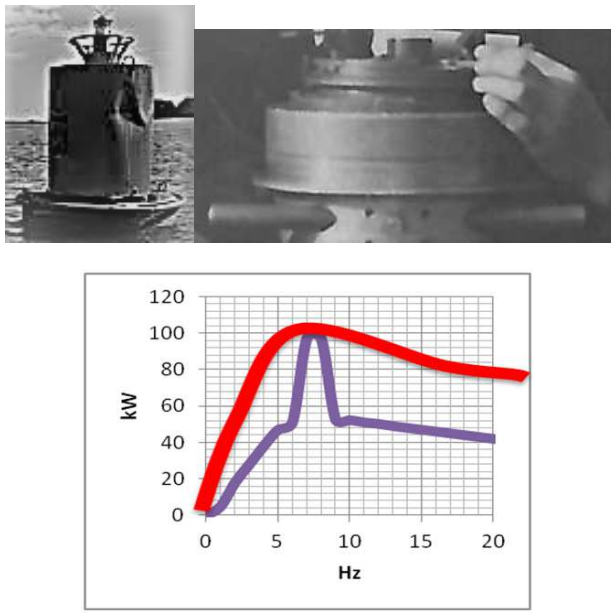

Figure 7. *Manufactured Buoy. Top photo of buoy, Middle photo- tuning. Bottom graph- 2 attempts to tune.*

The University also provided some measuring and

adjustment instrumentation for experimental work. There were several attempts for proper tuning (see right photo in top side of Figure 7) of buoy to get the electric power output 100 kW.

The graph shown in the bottom side of Figure 7 represents two attempts. The horizontal abscissa axis stands for frequency (in Hz), vertical ordinate axis stands for produced electric power.

As the target was to reach maximum 100 kW in frequency range 5 – 10 Hz, it can be stated that the buoy was tuned properly.

7. Results and Discussion

First of all it must be pointed out that there is no alternative for new invented VEHD for purpose of protection of ruined Mother Nature. The experimental tests prove for sure 100% effectiveness of proposed VEHD. The business behavior is brining closer and closer our planet Earth to a Point of No Return, when people would be disappearing.

The sad prognosis is 20-30 years. Why to wait?

Today all turbine and solar panel stations must be closed, also all fossil – fuel (including nuclear) stations must be stopped as soon as possible.

The Canadian Government has $ 9-10 billion to make that substitution real.

8. Conclusions

Based on unbeatable advantages of invented and patented Vibration Energy Harvesting Dampers it is right time to implement them in electric power generating industry. The perspective way to boost the efficiency of Wave Energy Harvesting Buoys is the equipping them by invented Vibration Energy Harvesting Dampers. The invented by authors Vibration Energy Harvesting Damper includes a support structure that is securable to a vibrating object, a tuned mass retained by the support structure and movable in a rectilinear direction, a magnet vibrationally coupled to and spaced apart from the tuned mass, a coil surrounding the magnet, and at least one biasing assembly connecting two or more of the support structure, the tuned mass and the magnet. The at least one biasing assembly includes a fixed biasing member and an adjustable biasing member arranged in parallel. The adjustable biasing member is configured to adjust the combined stiffness coefficient of the biasing assembly. The efficiency increase of Energy Harvesting Buoy is based on the properties of automatically controlled springing elements in the tuned mass dampers and that is adjustable to a broad range of frequencies of vibration.

The fabricated and tested sample of Wave Energy Harvesting Buoy could be the unit component on large system assembled from the similar units and can produce up to 500 MW of “green” electric power. Such assembly is a good example of environmentally friendly renewable technology for power generation.

The presented Wave Energy Harvesting Buoys with implanted Vibration Energy Harvesting Dampers could be used successfully in various marine situations allowing generates for free the significant amounts of electric energy.

Acknowledgements

The author pays a special tribute to National University of Shipbuilding, Nikolaev, Ukraine, for tremendous fantastic financial support.

References

[1] George Nerubenko, Cyril Nerubenko, Lucy Lebedeva, David Flowers, Volodymyr Gonchar, Roman Musiala, Moshe Michael Haimov, Dmytriy Gurevych “Vibration Energy Harvesting Damper”. U.S. Patent No. 10644579, May 05, 2020.

[2] George Nerubenko. Underwater Technique for Prevention of Oil Pollution. *Journal of Water Resources and Ocean Science.* Special Issue Safe Technology and Pollution Free Environment. Vol. 4, No. 1-1, 2015, pp. 1-10. doi: 10.11648/j.wros.s.2015040101.11.

[3] The EXXON VALDEZ Oil Spill. A Report to the President. From Samuel K. Skinner Secretary, Department of Transportation and William K. Reilly Administrator, Environmental Protection Agency. Prepared by The National Response Team May 1989.

[4] Office of Exxon Valdez Oil Spill (EVOS) Damage Assessment and Restoration. http://alaskafisheries.noaa.gov/oil/.

[5] Thomas Höfer. Tanker Safety and Coastal Environment: Prestige, Erika, and what else? ESPR – Environ Sci & Pollut Res 10 (1) 1–5 (2003). Ecomed publishers, D-86899 Landsberg, Germany and Ft. Worth/TX, USA • Tokyo, Japan • Mumbai, India Seoul, Korea.

[6] Curry L. Hagerty, Jonathan L. Ramseur. Deepwater Horizon Oil Spill: Selected Issues for Congress. Congressional Research Service. 7-5700. Report R41262. July 30, 2010. 48 p.

[7] Jonathan L. Ramseur, Curry L. Hagerty. Deepwater Horizon Oil Spill: Recent Activities and Ongoing Developments. Congressional Research Service. 7-5700. Report R42942. May 12, 2014. 16 p.

[8] Oil Spill Intelligence Report. Southern Cross University, Australia. Aspen Publishers. 2000.

[9] ITOPF. Oil Tankers Spill Statistics 2013. London, United Kingdom, 2014.

[10] Cheryl McMahon Anderson, Melinda Mayes, and Robert LaBelle. Update of Occurrence Rates for Offshore Oil Spills. OCS Report BOEM 2012-069 BSEE 2012-069. June 2012, 76 pages.

[11] Kerr, Richard A. (13 August 2010). A Lot of Oil on the Loose, Not So Much to Be Found. Science 329. (5993): 734–5. Bibcode: 2010 Sci 329.734 K. doi: 10.1126/science.329.5993.734. PMID 20705818.

[12] Dagmar Schmidt Etkin. Analysis of oil spill trends in the United States and worldwide. Proceedings, 2001 International oil spill conference. pp. 1291-1300.

[13] Stanislav Patin. Environmental Impact of the Offshore Oil and Gas Industry. Ecomonitor Pub; 1 edition (December 1, 1999), 448 pages.

[14] Hansen, J., Ruedy, R., Sato, M. & Lo, K. Global surface temperature change. *Rev. Geophys*. 48, RG4004 (2010).

[15] Serreze, M. C. & Barry, R. G. Processes and impacts of Arctic amplification: a research synthesis. *Glob. Planet. Change* 77, 85–96 (2011).

[16] Moon, T. A. et al. The expanding footprint of rapid Arctic change. *Earths Future* 7, 212–218 (2019).

[17] C Arden Pope 3rd, Richard T Burnett, Michelle C Turner, Aaron Cohen, Daniel Krewski, Michael Jerrett, Susan M Gapstur, Michael J Thun. Lung Cancer and Cardiovascular Disease Mortality Associated.

[18] George Nerubenko, Vladimir Blintsov, Andriy Mozgovyy, Ivan Biliuk. The Novel Wave Energy Harvesting Buoy. 2019 International Conference on Power Generation Systems and Renewable Energy Technologies (PGSRET), Istanbul, Turkey, DOI: 10.1109/PGSRET.2019.8882696.6 pages.

[19] Mathieu, E. (1868), "Mémoire sur Le Mouvement Vibratoired'une Membrane de forme Elliptique", Journal de Mathématiques Pures et Appliquées: 137–203.

[20] Arscott, Felix (1964). Periodic differential equations: an introduction to Mathieu, Lamé, and allied functions. Pergamon Press. ISBN 9781483164885.

[21] Stephen H. Davis and S. Rosenblat. A Quasiperiodic Mathieu-Hill Equation. SIAM Journal on Applied Mathematics Vol. 38, No. 1 (Feb., 1980), pp. 139-155 (17 pages).Published By Society for Industrial and Applied Mathematics.

[22] Francis M. Vanek, Louis D. Albright, Energy Systems Engineering. Evaluation and Implementation, McGraw-Hill Companies, Inc. 2008. 532 p.